Progress In Electromagnetics Research Letters, Vol. 131, 48–54, 2026

PIER Letters

(Received 27 April 2026, Accepted 13 July 2026, Scheduled 22 August 2026)

Design and Fabrication of a Wideband, Low-Cost, Lightweight Open TEM Cell

A. Monirihamedani*, M. R. Moniri Hamedani, and S. Hayati Raad

EMV Messtechnik GmbH, Wihelmstr. 95, 10117, Berlin, Germany

ABSTRACT: In this paper, a low-cost, lightweight open transverse electromagnetic (TEM) cell with an operating bandwidth from DC up to around 1.5 GHz is designed and fabricated. Initially, a fully metallic open cell is simulated, and associated TEM modes are exhibited by the spatial electric field distributions. The cell length (L_b), width (W_b), and height (H_b) are respectively 398, 200, and 103.93 mm. In the next step, a printed circuit board (PCB) is used as the septum to reduce the device's overall weight. Moreover, longitudinal slots are cut on both sides of the septum to prevent transverse currents, which results in the excitation of higher-order modes. For further weight reduction, sub-wavelength slots are cut in the metallic sidewalls without affecting the overall performance. The metal filling factor reduction is of great importance for reaching a portable test facility with reduced cost. Finally, the device's input ports are further manipulated to reduce discontinuity by gradually tapering them. The device is realized by the combination of metal sheet, computer numerical control (CNC) water jet, machining, and PCB technologies. The measured scattering parameters confirm the acceptable performance of the fabricated device.

1. INTRODUCTION

Transverse electromagnetic (TEM) cells are one of the critical devices for electromagnetic compatibility (EMC) tests. The EMC tests inside the TEM cells are conducted based on standardized procedures, including but not limited to IEC 61967-2, IEC 62132-2, and ISO 11452-3 automotive EMC tests [1–4]. These test facilities are employed for both radiation immunity and radiation emission tests in electronic systems, integrated circuits, digital systems, and wireless devices. They are employed in sensor calibration procedures and electromagnetic waves' biological effects [5, 6].

TEM cells are essentially formed by tapered rectangular coaxial lines with a rectangular strip line in between. The gradual transition between the connector and main waveguide improves device matching for extending the bandwidth [7–11]. These laboratories can be designed with either open or closed waveguide, with the former being more cost-effective [12]. Moreover, the operation of the TEM cell commonly relies on propagating TEM waves supported by strip-line waveguides. Recently, the evanescent modes excited by slotted rectangular waveguides have been employed in the design of a specific device for calibrating the spatial resolution of magnetic field probes [13].

The transverse wave field propagating inside the TEM cell resembles a plane wave to be potentially used as a simpler alternative to the plane wave propagation in open area test sites (OATSs) and anechoic chambers (AC) [13]. OATS testing can be cumbersome due to poor electromagnetic environments, large space requirements, and ground-plane mutual coupling and reflection effects. Shielded enclosures are not affected by these conditions, but they suffer from high construction cost, large space requirements, and potential inaccuracies due to supporting structures affecting equipment under test (EUT) performance [14, 15].

Compared with anechoic ranges, TEM cells offer a major advantage of enabling measurements at low frequencies below 1 GHz, a range that is difficult to cover in anechoic chambers. Importantly, their operating bandwidth starts from DC, since TEM-type electromagnetic waves have no cut-off frequency [16, 17]. Moreover, the transverse electromagnetic cells are cost-effective and do not require any antenna for measurement [18].

Due to their smaller test volume than shielded rooms, the same field strength can be generated with less power consumption [19]. Thus, susceptibility tests can be conducted with less power than free-space testing, and emission tests can be performed with an improved sensitivity inside the TEM cell [20]. The electric field intensity inside electromagnetic cells can be 3 V/m, 10 V/m, 30 V/m, or even higher, and it depends on the waveguide's geometry through the wave impedance of the waveguide and distance from the septum of the guide to the housing [21, 22].

As the circuits' operating frequency continues to increase, the presence of high-frequency currents and transient signals demands wideband test facilities [23]. The bandwidth of the TEM cells can be controlled by cross-section dimensions, location, and septum shape, and proper design of the "launch" parts [24]. The main barrier limiting the operating bandwidth of these cells is the emergence of higher-order modes and high-quality-factor cavity resonances in closed devices [25]. The

* Corresponding author: Alireza Monirihamedani (a.moniri@emvmetech.de).
www.emvmetech.de

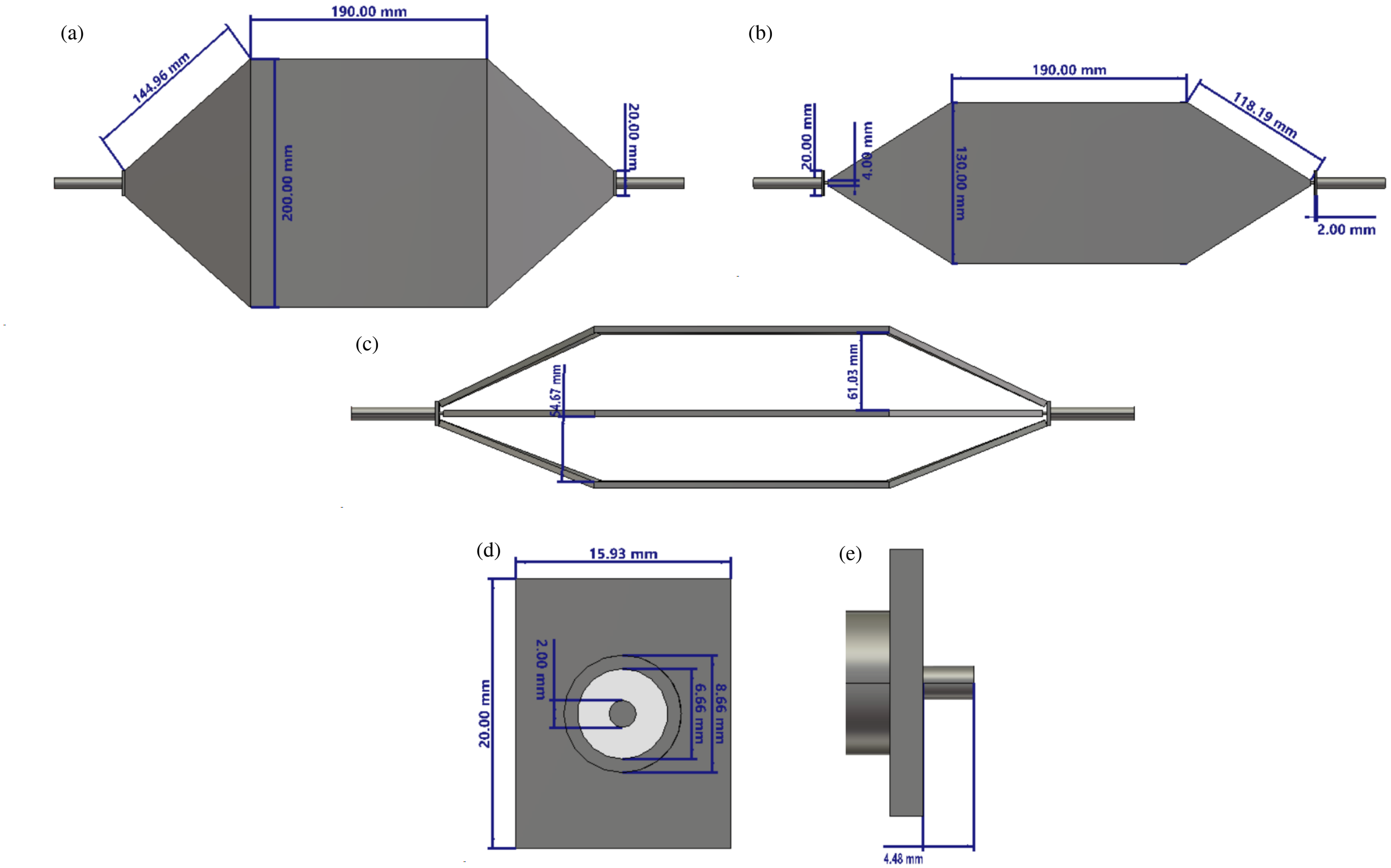

FIGURE 1. The geometry of the metallic open TEM cell excited by two coaxial cables: (a) top view, (b) septum, (c) side view, and (d)–(e) details of the feed.

cut-off frequencies of the higher-order modes can be estimated by a variety of methods, such as the transmission-line matrix (TLM) method or finite-element method (FEM) [26].

Different techniques have been proposed to suppress higher-order-mode contribution without affecting the propagation of transverse modes. These methods include the use of slotted walls, slotted septum, magnetic loops, ferrite tiles, and absorbing materials [27, 28]. Furthermore, segmented impedance matching, slitting the outer conductor, and adding an external shielding box are other techniques to extend operational bandwidths of TEM cells [29]. An advanced septum profile design is also developed to improve the device's impedance matching [30]. Note that using passive radio-frequency (RF) absorber materials for controlling higher-order mode amplitudes is only possible in large cells [31].

Given the significant advantages of open TEM cells, this paper presents a numerical analysis of such a device in Section 2. Due to the importance of slotted septum and slotted wall devices in providing multiple degrees of freedom for electromagnetic response manipulation, either by hollow slots or absorbing material-filled ones, Section 3 introduces some design guidelines for the low-cost, lightweight realization of the test facility by the slotting technique [27]. Modifying the mechanical structure for realization is also discussed in this section. Concluding remarks are mentioned in Section 4.

2. DESIGN PROCEDURE OF THE OPEN TEM CELL

In this section, the design procedure of the open TEM cell is discussed in detail. Specifically, the impact of the septum material on the device's operating bandwidth is provided. Later, the cell's transverse current reduction by inserting sub-wavelength slots in the septum is presented.

2.1. Open TEM Cell with Metallic Walls and Septum

In this section, the performance of an open TEM cell with metallic walls and a septum is provided. The top and side views of the proposed metallic test facility, along with the associated geometrical dimensions, are shown in Figs. 1(a)–(b). The structure is formed by an upper wall, a lower wall, and a central conductor (shown in Fig. 1(c)), and it is excited by two 50-ohm coaxial lines. The device is simulated in the CST software package using the time domain solver. The optimized geometrical parameters of the proposed cell are as follows: the cell length (L_b), width (W_b), and height (H_b) are, respectively, 398, 200, and 103.93 mm. Moreover, septum length (L_s), septum width (W_s), and septum height (H_s) are respectively 190, 130, and 54.67 mm. The metals are 4 mm-thick aluminum. Note that the commercially available dimensions of the wideband TEM cells are chosen as the initial values, and they are slightly modified via optimization to fit our fabrication constraints [32]. The TEM cell design equations can be found in [34].

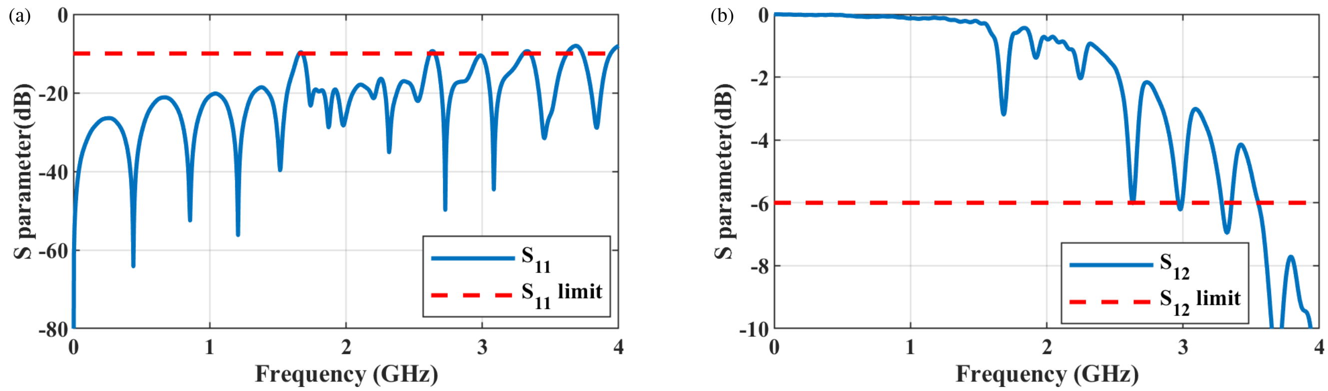

FIGURE 2. (a) S_{11} and (b) S_{12} of the metallic open TEM cell with the geometrical dimensions shown in Fig. 1.

Table 1. Spatial distributions of the electric field for the metallic TEM cell at three different frequencies. The rows are respectively dedicated to 1 GHz, 2 GHz, and 3 GHz frequencies.

f	E_x	E_y	E_z	
1 GHz	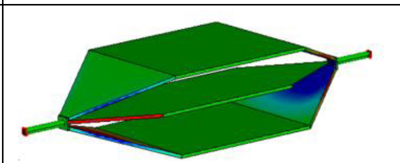	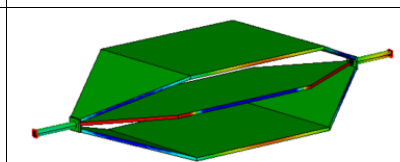	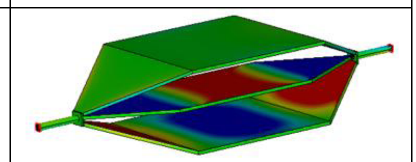	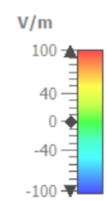
2 GHz	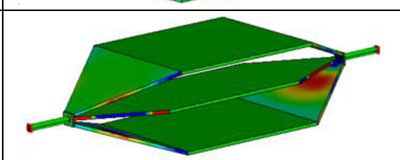	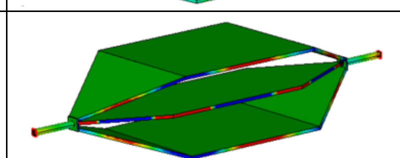	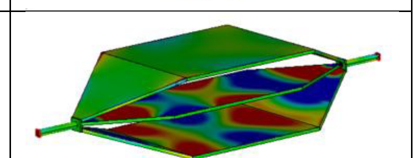	
3 GHz	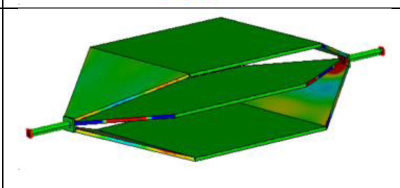	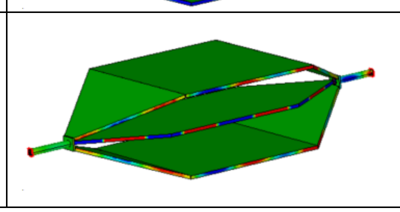	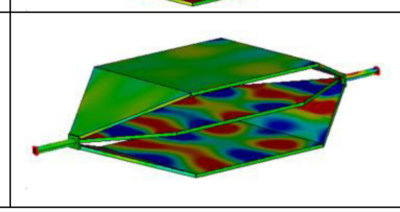	

Simulated scattering parameters of the TEM cell are shown in Fig. 2. Specifically, the S_{11} parameter is below -10 dB, and the S_{12} parameter is below -6 dB up to around 3.5 GHz. The aforementioned performance confirms the device's proper operation, since reflection and absorption losses are negligible, and most of the energy is transmitted to the second port.

Spatial distributions of the electric field at three different frequencies (1, 2, and 3 GHz) are summarized in Table 1. The figures show that the E_x and E_y components are negligible compared to the E_z wave field. Thus, higher-order transverse electric (TE) and transverse magnetic (TM) modes are suppressed in the operating band via the proper choice of dimensions.

2.2. Open TEM Cell with Metallic Walls and Slotted PCB Septum

In the next step, the metallic septum is replaced by a PCB septum in the simulation to reduce weight. The height of the FR4 substrate with a permittivity of $\varepsilon_r = 4.3$ and loss tangent of $\tan\delta = 0.025$ is considered to be the same as the metallic septum, and it is between two 35 µm copper layers. The scattering parameters of the TEM cell with PCB septum are shown in Fig. 3. Based on the results, with the PCB septum, the same performance as the metallic septum is obtained.

To further improve the performance of the test facility, a slotted septum as in Fig. 4(a) is used. Specifically, 7 slots are cut on both sides of the septum to prevent the propagation of the transverse currents by disturbing their propagation path [27]. These slots have a negligible impact on longitudinal currents. The widths of the slots are 4 mm in the rectangular section, and they are tapered to zero in the other sections. The scattering parameters of the device with the slotted PCB septum are illustrated in Fig. 4(b), confirming the priority of the slotted septum.

3. FABRICATION OF AN OPEN TEM CELL

In the previous section, the performance of an open TEM cell with a slotted dielectric septum is verified numerically. To achieve a lightweight design, 13 slots are cut in the device sidewalls. The width of the slots is 4 mm, resulting in around 38% weight reduction in each rectangular section. The slots are electrically small in the whole operating spectrum, ensur-

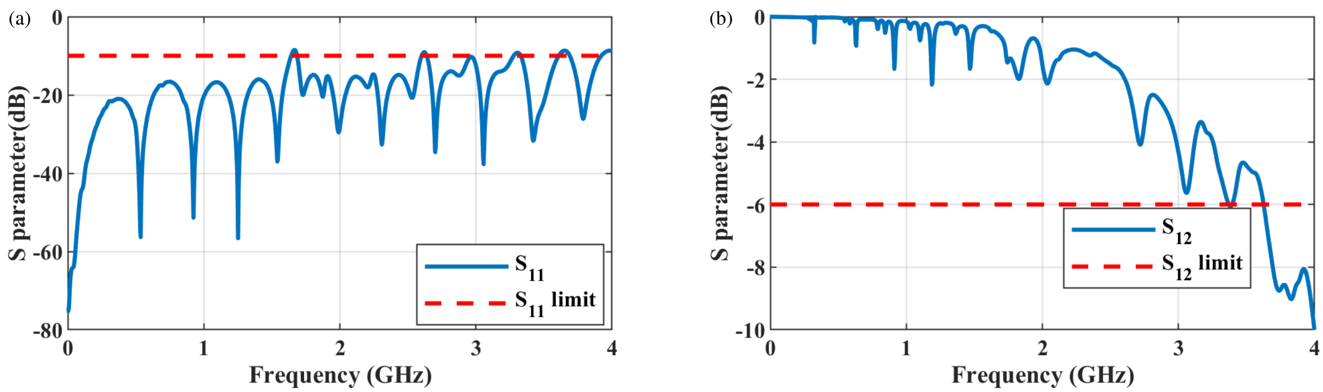

FIGURE 3. (a) S_{11} and (b) S_{12} of the open TEM cell considering a PCB septum with the same height as the metallic septum in Fig. 1.

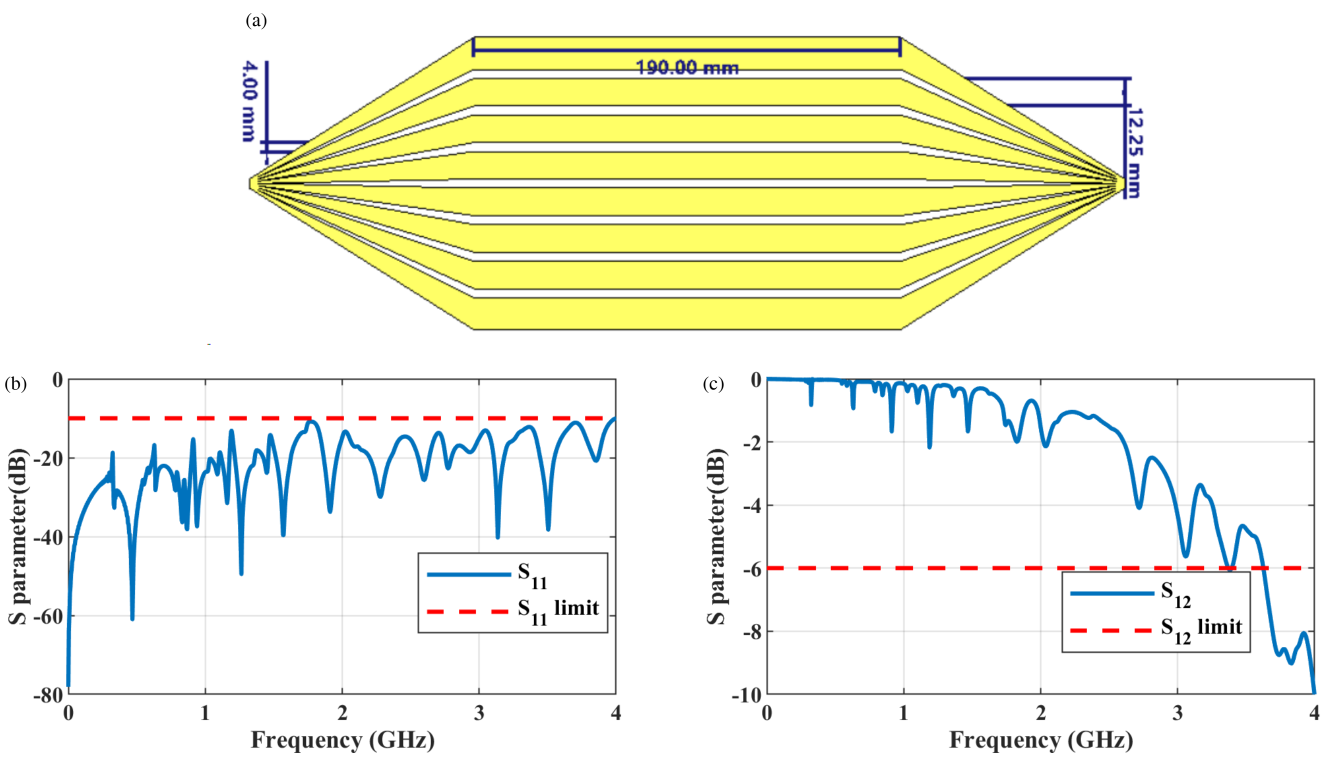

FIGURE 4. (a) The schematic of the slotted PCB septum and (b)–(c) scattering parameters of the open TEM cell with slotted PCB septum.

ing minimal power loss due to leakage. These modifications aid in reaching lightweight portable devices, reduce cost due to the lower metal filling factor, and offer the chance for performance controlling by installing resistors or adding absorbing materials in gaps. The final structure is illustrated in Figs. 5(a)–(b). There were some necessary geometry modifications such as adding holder to the bottom of the device to ensure its mechanical stability, adding slightly curved connecting sections between the rectangular and tapered parts as in Fig. 5(a), adding curved connecting parts as in Fig. 5(d), adding the connector and its screws to the electromagnetic model, and increasing the taper width from zero to 2 mm in the transition section to make its realization feasible. Thus, the geometrical dimensions are optimized to compensate for these effects. The new dimensions are shown in Fig. 5. Moreover, input and output ports are N-type female connectors with an inner conductor radius of 1 mm and an outer conductor radius of 3.33 mm. The mechanical prototype cross-sectional view is shown in Fig. 5(c), and the tapered conical section in Fig. 5(d) is considered for wideband impedance matching. For improving impedance matching, gradual tapering is considered in the input of the septum, as illustrated in Fig. 5(d).

The device is fabricated using sheet metal technology. The slots in the side walls are realized by water-jet CNC. Moreover, the septum is fabricated using PCB technology, and the remaining parts are realized with machining. The final fabricated structure is shown in Fig. 6(a), and its scattering parameters are compared with those of the simulated structure. Good agreement is achieved between the simulated and measured results up to 1.4 GHz. Thus, our proposed device can be used for conducting reliable EMC tests. There is a considerable disparity between the bandwidths of simulated and measured de-

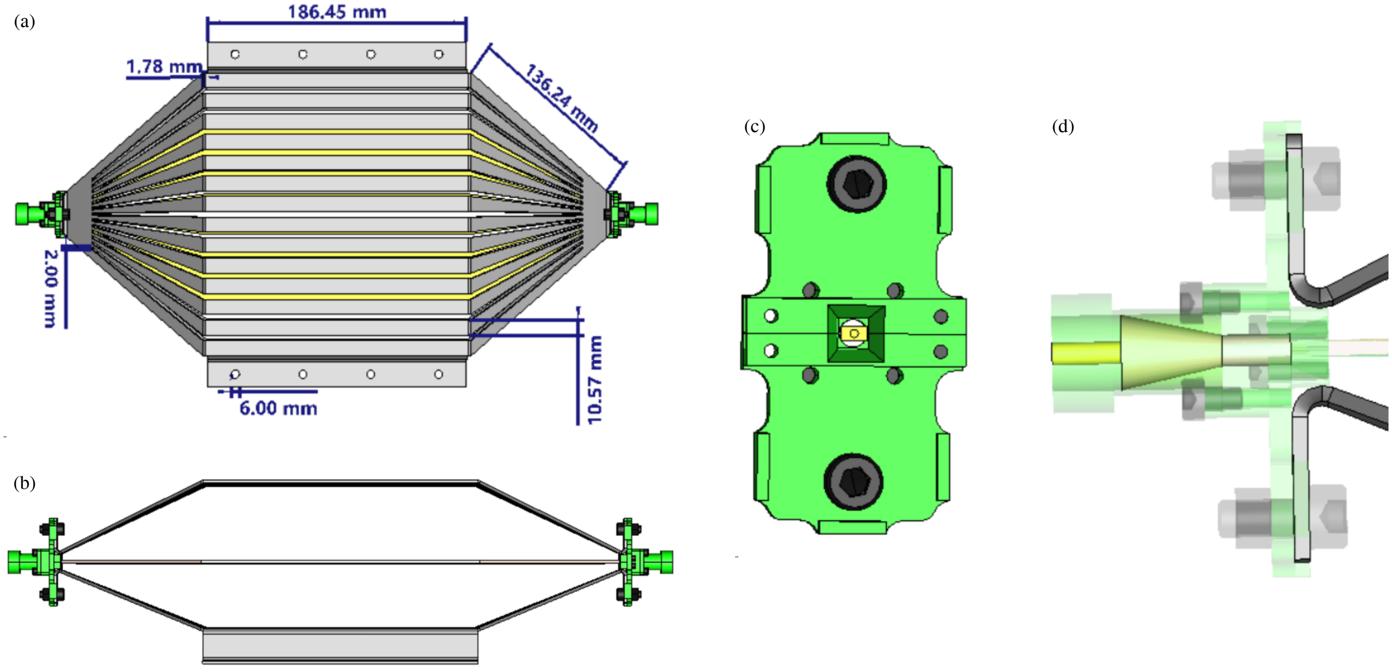

FIGURE 5. (a) Top and (b) side views of the final version of the proposed open TEM cell with slotted wall and septum. (c) The cross-sectional view of the N-type connector holder and (d) the designed tapered input section for impedance matching improvement.

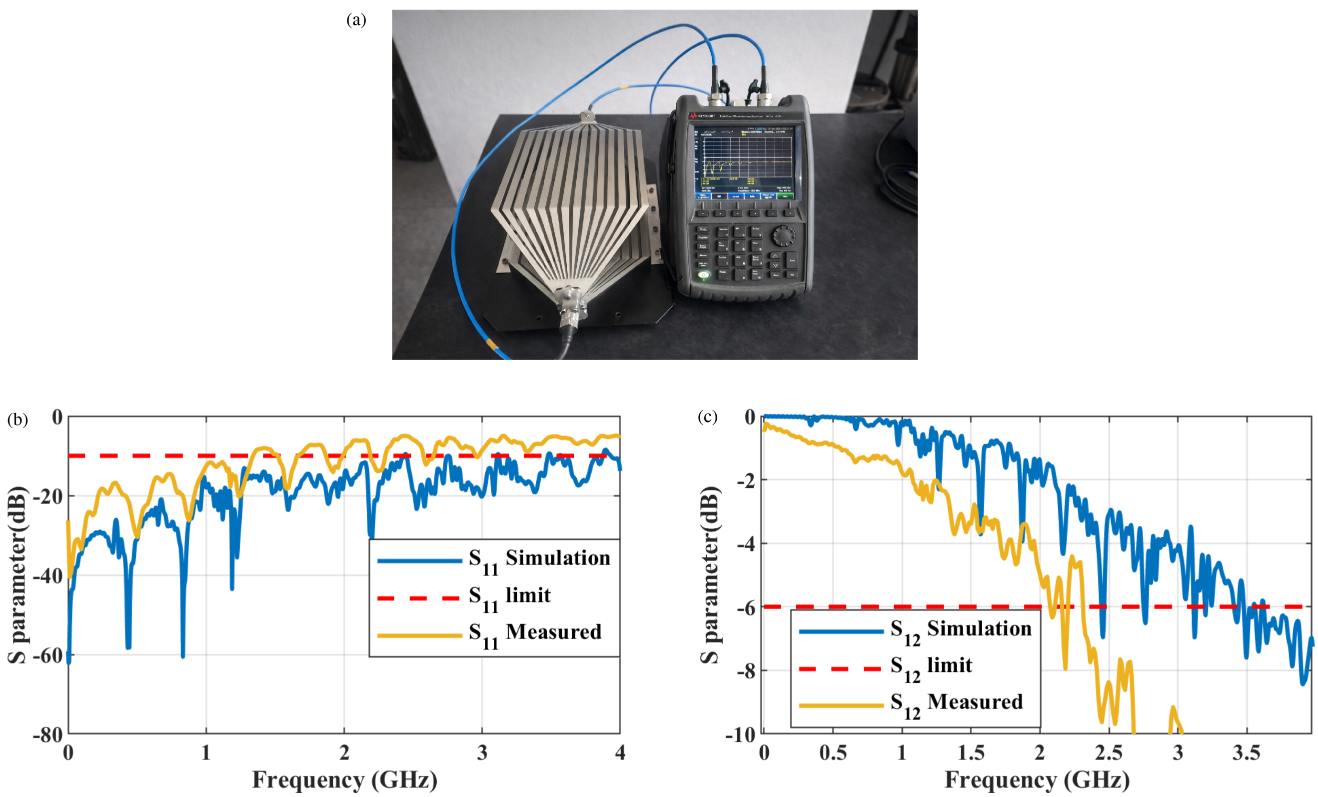

FIGURE 6. (a) Fabricated prototype of our proposed TEM cell and (b)–(c) its simulated and measured scattering parameters.

vices. The fabrication imperfections and the lack of a shield box might be possible reasons for this issue. Specifically, the originally considered homogeneous slots on the side walls are not achieved with the employed fabrication methods. Moreover, due to the lack of a connector model, the final optimized dimensions and simulation results are provided by available connector models. There were also some size disparities between the fabricated device and simulated one. Despite all these factors, the device still performs in a bandwidth of around 1.5 GHz. Fabrication tolerance analysis and using the space provided by the

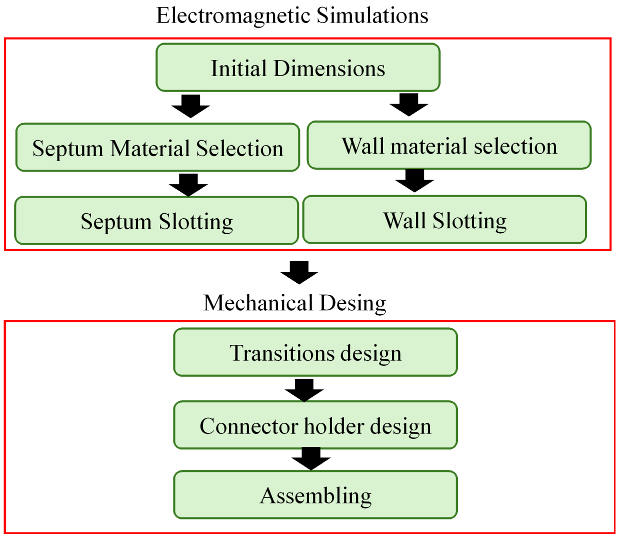

FIGURE 7. The design procedure flowchart.

slots for bandwidth enhancement will be considered in future work.

Finally, the design procedure flowchart is shown in Fig. 7. As the figure shows, the mechanical design is crucial for the proposed device due to its complex geometry. The device's advantages can be summarized as follows:

1) Reaching a lightweight portable device by using a PCB septum and reducing the metal filling factor in walls.

2) Achieving different degrees of freedom (either by optimizing the slot dimensions or adding resistors or absorbing materials to the air in future designs).

3) Confirming the possibility of device fabrication using the conventional techniques to realize the slotted geometry (to be further improved by the fabrication tolerance analysis).

4. CONCLUSIONS

By properly selecting geometrical dimensions of the open TEM cell, its operating bandwidth can be tuned. Moreover, by inserting longitudinal slots on the device's PCB septum, higher-order-mode propagation can be prohibited. It is observed that by inserting multiple subwavelength slots on metallic sidewalls, a lightweight portable device can be achieved, offering the same performance as a slot-less device. The mechanical design is a key part of designing slotted TEM cells, and fabrication tolerance analysis should be conducted in future work.

REFERENCES

[1] Mandic, T., R. Gillon, B. Nauwelaers, and A. Baric, "Characterizing the TEM cell electric and magnetic field coupling to PCB transmission lines," *IEEE Transactions on Electromagnetic Compatibility*, Vol. 54, No. 5, 976–985, 2012.

[2] Koohestani, M., M. Ramdani, P. Besnier, J.-L. Levant, and R. Perdriau, "Perturbations of electric and magnetic fields due to the presence of materials in TEM cells," *IEEE Transactions on Electromagnetic Compatibility*, Vol. 62, No. 4, 997–1006, 2020.

[3] Trip, R., A.-M. Silaghi, A. Buta, and A. D. Sabata, "TEM cell measurements in automotive EMC: A case study," in *2022 International Symposium on Electronics and Telecommunications (ISETC)*, 1–4, Timisoara, Romania, 2022.

[4] Hayati Raad, S., "Analysis and design of absorbers for electromagnetic compatibility applications," in *Electromagnetic Compatibility*, 2021.

[5] Wang, S., S. Fang, and P. Chen, "Design and optimization of a wideband rectangular TEM device for cell experiments," *Applied Computational Electromagnetics Society Journal (ACES)*, Vol. 37, No. 1, 85–92, 2022.

[6] Soueid, M., S. Kohler, L. Carr, S. M. Bardet, R. P. O'Connor, P. Leveque, and D. Arnaud-Cormos, "Electromagnetic analysis of an aperture modified TEM cell including an ITO layer for real-time observation of biological cells exposed to microwaves," *Progress In Electromagnetics Research*, Vol. 149, 193–204, 2014.

[7] Al Takach, A., F. Ndagijimana, J. Jomaah, and M. Al-Husseini, "3D-printed low-cost and lightweight TEM cell," in *2018 International Conference on High Performance Computing & Simulation (HPCS)*, 47–50, Orleans, France, 2018.

[8] Das, B. N. and S. A. Mohan, "Analysis of a TEM cell with septum on a dielectric slab," *IEEE Transactions on Electromagnetic Compatibility*, Vol. EMC-27, No. 1, 1–6, 1985.

[9] Hill, D. A., "Bandwidth limitations of TEM cells due to resonances," *Journal of Microwave Power*, Vol. 18, No. 2, 181–195, 1983.

[10] Demakov, A. V. and M. E. Komnatnov, "TEM cell for testing low-profile integrated circuits for EMC," in *2020 21st International Conference of Young Specialists on Micro/Nanotechnologies and Electron Devices (EDM)*, 154–158, Chemal, Russia, 2020.

[11] Yildiz, C., G. Demirel, and F. Çalışkan, "Designing transverse electromagnetic (TEM) cell," in *3rd Electromagnetic Compatibility Conference (EMC TURKIYE)*, 2015.

[12] Ambati, B. N., V. R. Botsa, S. K. Munaka, and S. Bandaru, "Modeling, simulation & validation of TEM cell for short pulse sensor verification," in *2018 15th International Conference on ElectroMagnetic Interference & Compatibility (INCEMIC)*, 1–4, Bengaluru, India, 2018.

[13] Karst, J. P., C. Groh, and H. Garbe, "Calculable field generation using TEM cells applied to the calibration of a novel E-field probe," *IEEE Transactions on Electromagnetic Compatibility*, Vol. 44, No. 1, 59–71, 2002.

[14] Groh, C., J. P. Karst, M. Koch, and H. Garbe, "TEM waveguides for EMC measurements," *IEEE Transactions on Electromagnetic Compatibility*, Vol. 41, No. 4, 440–445, 1999.

[15] Jiang, K., Y. Huang, S. Shen, X. Chen, and Y. Xie, "Source-stirred method for total radiated power measurements in a TEM cell," *IEEE Transactions on Antennas and Propagation*, Vol. 73, No. 4, 2192–2203, 2025.

[16] Moirioka, T., S. Kurokawa, Y. Toba, and J. Ichijyo, "Precision E-field uniformity measurement of a probe loaded TEM cell using an optical probe," in *2016 URSI Asia-Pacific Radio Science Conference (URSI AP-RASC)*, 1–3, Seoul, Korea (South), 2016.

[17] Satav, S. M. and V. Agarwal, "Do-it-yourself fabrication of an open TEM cell for EMC pre-compliance," *IEEE Emc Society Newsletter*, Vol. 218, 66–71, 2008.

[18] Budania, M., G. Verma, and A. Jeyakumar, "Design and analysis of GTEM cell using CST studio simulation," in *2020 IEEE International Conference on Electronics, Computing and Communication Technologies (CONECCT)*, 1–5, Bangalore, India, 2020.

[19] Chechetkin, V., A. Korotkov, and V. Kozlov, "Investigation of the characteristics of the TEM cell prototype," in *2019 International Multi-Conference on Engineering, Computer and In-*

formation Sciences (SIBIRCON), 241–244, Novosibirsk, Russia, 2019.

[20] Koohestani, M., M. Ramdani, F. Lafon, A. A. Moreira, and R. Perdriau, "Impact of field polarization on radiated emission characterization in an open TEM cell," *IEEE Transactions on Instrumentation and Measurement*, Vol. 69, No. 9, 6595–6602, 2020.

[21] Malaric, K. and I. Bacic, "Efficiency of the materials used in building TEM-cell," in *2008 14th Conference on Microwave Techniques*, 1–3, Prague, Czech Republic, 2008.

[22] Kreindl, D., T. Bauernfeind, B. Weiss, C. Stockreiter, and M. Kaltenbacher, "Evaluation of an analytical equivalent hertzian dipole representation in tem cells applying the finite element method," *IEEE Transactions on Magnetics*, Vol. 60, No. 3, 1–4, 2024.

[23] Chen, L., J. Wu, H. Zhang, Y. Zheng, and J. Wu, "An optimized test method based on IC-Stripline TEM Cell," in *2021 Asia-Pacific International Symposium on Electromagnetic Compatibility (APEMC)*, 1–4, Nusa Dua-Bali, Indonesia, 2021.

[24] Gu, Y., Z. Zhou, J. Ren, M. Sheng, and Q. Zhou, "Calculation of ATEM cell characteristic impedance based on static field approximation and MoM," *IEEE Transactions on Electromagnetic Compatibility*, Vol. 66, No. 3, 694–705, 2024.

[25] Gu, Y., Z. Zhou, and M. Sheng, "Design and Development of a TEM Cell up to 1 GHz," in *2020 6th Global Electromagnetic Compatibility Conference (GEMCCON)*, 1–4, Xi'an, China, 2020.

[26] Pham, H. D., K. Tüting, and H. Garbe, "Concept to evaluate and quantify field inhomogeneities in coaxial TEM-cells," *IEEE Transactions on Instrumentation and Measurement*, Vol. 70, 1–14, 2021.

[27] Deng, S., D. Pommerenke, T. Hubing, and D. Shin, "An experimental investigation of higher order mode suppression in TEM cells," *IEEE Transactions on Electromagnetic Compatibility*, Vol. 50, No. 2, 416–419, 2008.

[28] Deng, S., D. Pommerenke, T. Hubing, J. Drewniak, D. Beetner, D. Shin, S. Kim, and H. Kwak, "Mode suppressed TEM cell design for high frequency IC measurements," in *2007 IEEE International Symposium on Electromagnetic Compatibility*, 1–6, Honolulu, HI, USA, 2007.

[29] Zhou, T., X. Peng, S. Huang, J. Zhao, and H. Sun, "Design and optimization of a TEM cell structure suitable for wider bandwidth," *Progress In Electromagnetics Research M*, Vol. 106, 93–104, 2021.

[30] Giannetti, G., C. Spindelberger, and H. Arthaber, "Simple semi-analytical septum design for improved matching in open TEM cells," *IEEE Letters on Electromagnetic Compatibility Practice and Applications*, Vol. 6, No. 1, 6–10, 2024.

[31] Walters, A. J. and C. Leat, "Control of the TE_{111} resonance inan asymmetric TEM cell," *IEEE Transactions on Electromagnetic Compatibility*, Vol. 50, No. 2, 431–434, 2008.

[32] Open TEM Cells for EMC Pre-Compliance Testing, https://www.tekbox.com/product/open-tem-cells-emc-compliance-testing/.

[33] Iftode, C. and S. Miclaus, "Design and validation of a TEM cell used for radiofrequency dosimetric studies," *Progress In Electromagnetics Research*, Vol. 132, 369–388, 2012.